Magnetic polarization of noble metals by Co nanoparticles in *M*-capped granular multilayers (*M*=Cu, Ag, and Au): An x-ray magnetic circular dichroism study

J. Bartolomé,[1] L. M. García,[1] F. Bartolomé,[1] F. Luis,[1] R. López-Ruiz,[1] F. Petroff,[2] C. Deranlot,[2] F. Wilhelm,[3] A. Rogalev,[3] P. Bencok,[3] N. B. Brookes,[3] L. Ruiz,[4] and J. M. González-Calbet[4]

[1]*Instituto de Ciencia de Materiales de Aragón and Departamento de Física de la Materia Condensada, CSIC-Universidad de Zaragoza, 50009 Zaragoza, Spain*

[2]*Unité Mixte de Physique CNRS/Thales, Route Départementale 128, 91767 Palaiseau Cedex, France and Université Paris-Sud, 91405 Orsay Cedex, France*

[3]*European Synchrotron Radiation Facility, Boite Postale 220, F-38043 Grenoble, France*

[4]*Departamento de Química Inorgánica, Universidad Complutense de Madrid, E-28040 Madrid, Spain*

(Received 8 November 2007; revised manuscript received 14 March 2008; published 15 May 2008)

X-ray magnetic circular dichroism spectra have been recorded at the $L_{2,3}$ edges of Co, Cu, Ag, and Au, and at the *K* edges of Co and Cu for a series of multilayer systems of partially self-assembled Co nanoparticles, both capped with alumina and with different metals (Cu, Ag, and Au). The orbital and spin moments m_L and m_S and their ratio m_L/m_S, for Co, Cu, Ag, and Au, have been determined from those measurements. The trend of increasing m_L/m_S for Co is the same as found for increasing the effective anisotropy K_{eff} alumina $<$Cu $<$Ag$<$Au capped. It is shown that the relative increase in the surface contribution for both quantities, $(m_L/m_S)_{\text{surf}}$ and K_S, is directly correlated. It is argued that the increase in m_L with metal capping actually reflects an increase in the anisotropy of the orbital moment for the Co surface atoms. The redistribution of the number of holes in the noble metal bands by hybridization with the Co surface atom 3*d* band and the polarization of the *nd* band by exchange interaction with the Co bands give rise to the magnetic moments derived for the three noble metals investigated.

DOI: 10.1103/PhysRevB.77.184420 PACS number(s): 75.50.Tt, 75.20.−g, 75.30.Gw, 73.22.−f

I. INTRODUCTION

Decreasing the size of particles to the nanometric scale leads to a preponderance of the number of surface atoms with respect to the core ones. In many cases, the particles are embedded in a supporting matrix or covered by a shell of different composition. Therefore, the interface atoms of the particle and the environment are expected to play an important role in the magnetic properties of each individual particle and, hence, of the system formed by the ensemble of particles, surrounding shell and interparticle connecting matter.

A good example of the previous statement is a system consisting of metallic Co nanoparticles with average diameter $\langle D\rangle$ in the range of 1–4 nm, embedded in amorphous alumina. The energy barrier hindering the reversal of the magnetic moment is $U=K_{\text{eff}}V$ for not-interacting particles, where K_{eff} is the magnetic anisotropy effective constant. It has been experimentally shown that K_{eff} inversely depends on $\langle D\rangle$,

$$K_{\text{eff}} \cong K_{\text{bulk}} + \frac{6K_S}{\langle D\rangle}, \tag{1}$$

where K_S is the magnetic surface anisotropy constant.[1] For the particles in the aforementioned range of diameters, the surface contribution is dominant. This expression has been empirically accepted as a proof of the dominating effect of surface anisotropy, although a note of attention should be mentioned; in a recent theoretical work, this expression has been found to be fulfilled by Co particles only when there is a certain elongation in the particle shape.[2]

Another quantity that has been found to depend on the Co particle average diameter is the ratio of orbital moment with respect to spin moment m_L/m_S, as determined from x-ray magnetic circular dichroism (XMCD) measurements.[3] The Co particles embedded in alumina also show the same inverse relationship to $\langle D\rangle$.[4] Therefore, K_{eff} and m_L/m_S seem to be correlated and dependent on the particle size.

In a previous work, it was shown that the interface between the particle and the surrounding matrix could be modified by capping the Co nanoparticles with Cu or Au. The cap completely surrounds each particle, therefore it effectively modifies the matrix in which the particle is embedded. In both cases, K_{eff} increased with respect to the value for the alumina-capped particles, with the trend $K_{\text{eff}}^{\text{Al}_2\text{O}_3} < K_{\text{eff}}^{\text{Cu}} < K_{\text{eff}}^{\text{Au}}$.[5–7] Likewise, an increase in the Co m_L/m_S could be observed for the two capping cases, increasing with the same trend.[6,7] Varying the matrix seems to have, therefore, a strong impact on K_{eff}.

In this work, the noble metals Cu, Ag, and Au have been used to cap the Co particles, and to modify in this way the matrix in which the particles are embedded, from the insulating case of Al_2O_3 to the conducting case of metals, while maintaining all the other parameters. In this way, dipolar interactions may be assumed to contribute to the *U* by a similar amount, while exchange interactions are too short ranged to modify it.[7] Therefore, to study the interface effects Co granular multilayers, with the same average diameter $\langle D\rangle=3$ nm and interparticle distances, have been studied as a function of capping substitution. These metals have nearly filled $3d^{10}$, $4d^{10}$, and $5d^{10}$ bands and are diamagnetic in the absence of any hybridization.

It is known from studies on Co thin films capped with Cu and Au that the interface plays a paramount role in the modification of the surface anisotropy[8] and that the noble metals (Cu, Ag, or Au) become polarized by the magnetic Co.[9–12]

Although the three metals share a d^{10}-type band, the *nd* spin-orbit coupling differs by a factor of 6 from Cu to Au, and the Fermi energy also markedly differs. Therefore, the interactions of the *nd* band electrons with the Co surface atoms can be systematically modified. The same interactions should be effective in the capped Co nanoparticles, so it was deemed interesting to study the resulting variations of the particle magnetic properties to gain information on the mechanism giving rise to an enhancement of the anisotropy. Because of the element selectivity and high sensitivity of the present XMCD setups, this technique has been applied to obtain information on the orbital and spin moment components of the Co and the capping metals independently.

II. EXPERIMENT

The samples are prepared by sequential sputtering on a Si substrate of amorphous alumina buffer layer, Co, and the capping material, either alumina, Cu, Ag, or Au. The formation of Co aggregates on the amorphous alumina is the result of three-dimensional growth because of the different surface energies between alumina and Co. The metal and alumina are deposited using Ar plasma at a radio frequency power of 100 W. The substrate temperature is kept constant at 293 K and the Ar pressure is 4×10^{-3} Torr. Co aggregates are formed with $\langle D\rangle$, which linearly depends on the nominal thickness t_{Co} that the layer would have if it was continuous, i.e., on the Co deposition time. $\langle D\rangle$ can be changed in the range $0.7<\langle D\rangle<5$ nm with a guarantee that the particles do not touch one another.[13,14] The alumina or metal capping layer deposited on the so formed particles completely surrounds each particle (see below), therefore it can be envisaged as a matrix in which the particle is embedded. It is described by its nominal thickness t_M. On top of the capping layer, a new alumina layer is deposited to act subsequently as generator of the new layer of Co particles. It is interesting to note that, at least for some of the thicknesses, the new particles predominantly form in the valleys created by the previous granular layer.[15] The process may continue until the desired number of trilayers N is obtained, which was $N\approx20$ in the present samples for XMCD experiments. The samples consisted of platelets of 1×1 cm^2.

The transmission electron microscopy (TEM) study was carried out with a JEOL 3000FEG electron microscope fitted with an Oxford LINK electron dispersive spectrometry analyzer. Cross-sectional TEM specimens were prepared by gluing two films face to face, followed by slicing, grinding, polishing, and dimpling. Special care was taken to avoid irradiation damage during ion milling by working at a low angle (7°) and a low voltage (3.5 kV) and by cooling the sample using liquid nitrogen.

The x-ray absorption spectroscopy (XAS) and XMCD experiments have been performed at the European Synchrotron Radiation Facility (ESRF) in Grenoble at the ID08 (Cu and Co $L_{2,3}$ edges) and at the ID12 (Co and Cu K edges, and Ag and Au $L_{2,3}$ edges) beamlines. At the ID08 beamline, an APPLE-II undulator and a spherical grating monochromator were used. The degree of polarization was ~100%. The total electron yield detection method was employed. The beam direction, parallel to the applied magnetic field, had an incident angle of 15° with respect to the normal to the plate.

At the ID12 beamline, the undulators APPLE-II and Helios II were employed, and a double-Si(111)-crystal monochromator provided a monochromatized beam. The polarization was over 90% in all cases, except at the energies of the Ag L_2 and L_3 edges where it was 36% and 24%, respectively. The detection technique used in the ID12 experiments was fluorescence in backscattering geometry. The XMCD signal was obtained by a direct difference of the XAS spectra recorded with opposite helicities at each fixed magnetic field value for both orientations of the field. The applied field was 1 T and the temperature was $T=5$ K in all cases. The field was applied with an incident angle of 75° with respect to the normal to the plate. The data shown for Ag and Au are the average of several tens of independent measurements

The coercive field extracted from magnetic hysteresis data at any temperature is isotropic. Therefore, there is no evidence of the capping inducing any preferred orientation for the anisotropy axis. This supports our assumption that the particles can be described well in terms of an average diameter $\langle D\rangle$. The effective magnetic average diameter is determined from the analysis of the magnetization $M(H)$, fitting it to the Langevin function for a particle with diameter D, averaged over a Gaussian distribution of D, and the susceptibility $\chi(T)$ for Curie–Weiss behavior averaged in the same way. The procedure has been extensively described in Ref. 1. Once the magnetic average diameter has been determined, a scaling analysis of the out-of-phase susceptibility χ'' yields the distribution of activation energies U for a given sample. Then, knowing the distributions of D and U, one accurately derives $K_{\mathrm{eff}}=6U(\langle D\rangle)/(\pi\langle D\rangle^3)$.[1,7]

The samples which were measured had an average Co particle diameter of $\langle D\rangle=3$ nm, except in the case of Au capping in which a sample with $\langle D\rangle=1.8$ nm was also measured. The XAS spectra at the Co L_3 edge of all the samples reported [see Fig. 5(a), as an example] are characteristic of metallic Co; i.e., we do not observe any prepeak, or shoulder above the peak, distinctive of the presence of Co-O bonds.[16] Therefore, we are quite sure that the Co particles are not oxidized during the fabrication process.

III. MORPHOLOGICAL AND STRUCTURAL CHARACTERIZATION

The morphological and structural characteristics of the Co particles, which are embedded in alumina, had been previously studied in detail by TEM, extended x-ray absorption fine structure, and x-ray diffraction.[13–17] It has been shown[14,18] that Co particles with $\langle D\rangle<3$ nm ($t_{\mathrm{Co}}<0.8$ nm), as is the present case, crystallize in the fcc phase, while for t_{Co} higher than that threshold, they crystallize in the hcp structure. The particles are well separated from each other and form a multilayer system of Co particles. Besides, the Co fraction that does not coalesce into particles remains in the matrix in atomic form, or in very small clusters of a few atoms.[13] The nonaggregated Co is described by the parameter x_{para} because of its paramagnetic contribution to the sample magnetism at all temperatures, and it has been evaluated from the

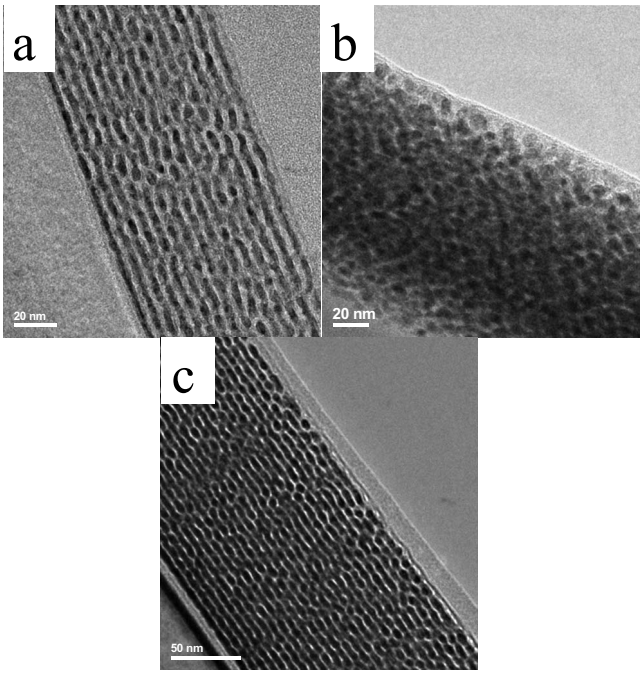

FIG. 1. TEM cross sections of granular multilayers with $t_{Co}=0.7$ nm, $t_M=1.5$ nm, and $t_{Al_2O_3}=3$ nm. (a) $Si/Al_2O_3/(Co/Cu/Al_2O_3)\times 15/Al_2O_3$, (b) $Si/Al_2O_3/(Co/Ag/Al_2O_3)\times 20/Al_2O_3$, and (c) $Si/Al_2O_3/(Co/Au/Al_2O_3)\times 25/Al_2O_3$. The dark spots correspond to the Co particles covered by the noble metal. The intermediate light area is the amorphous Al_2O_3.

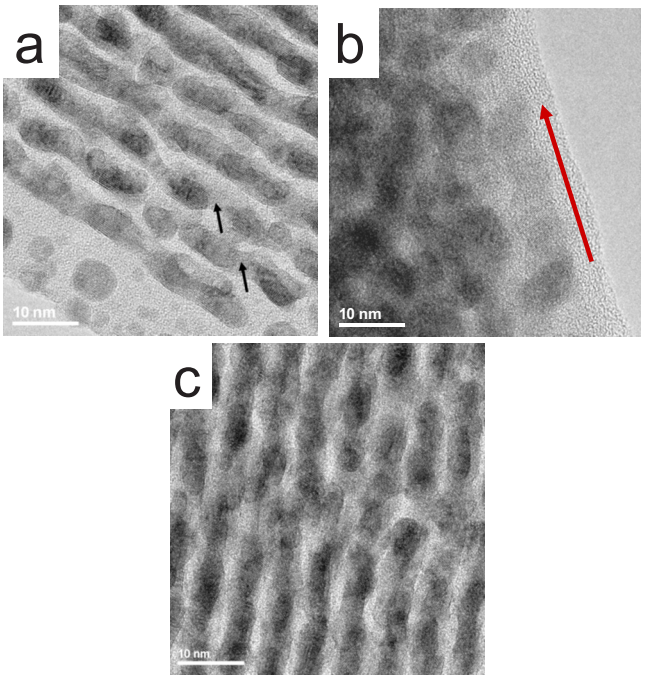

FIG. 2. (Color online) HRTEM cross sections of the same samples as in Fig. 1: (a) Cu, (b) Ag, and (c) Au capped. In the Co/Cu and Co/Au cases, the dark granular layers are now resolved into segregated particles at the border of the dimple. The Co particles are surrounded and interconnected by the lighter gray M capping [arrows in (a)]. Some peanut-shaped double particles reflect the superposition of the projection of particles in the transmission measurement. The arrow in (b) indicates a row of particles in one of the layers at the dimple border.

difference between the nominal Co deposition and a direct count of Co clusters from plane view TEM, resulting in Co/Al_2O_3 samples that are $x_{para}=77\%$ and 45% for the $t_{Co}=0.4$ and 0.7 nm samples, respectively. Indirectly, x_{para} has been deduced from $M(H)$ measurements, yielding the values $x_{para}=50\%$ and 25% for the $t_{Co}=0.4$ and $t_{Co}=0.7$ nm samples, respectively.[13,19] Note that these values somewhat differ from the more direct results obtained from the TEM measurements for Co/Al_2O_3 samples.

To assess the morphology and number of layers of the films, a TEM study has been performed on cross sections of the Cu-, Ag-, and Au-capped multilayers, with nominal thicknesses $t_{Co}=0.7$ nm, $t_M=1.5$ nm, and $t_{Al_2O_3}=3$ nm. In Fig. 1(a), the image of the $Si/Al_2O_3/(Co/Cu/Al_2O_3)\times 15/Al_2O_3$ sample shows an ordered arrangement of 15 dark and bright fringes of 4 and 1.2 nm average thicknesses, respectively, which perfectly agrees with the nominal sequential layer deposition in the system. A similar dark (3.5 nm) and bright (2.5 nm) fringe distribution is observed for the $Si/Al_2O_3/(Co/Au/Al_2O_3)\times 25/Al_2O_3$ system where 25 layers are evident [Fig. 1(c)]. In both cases, the dark fringes are apparently built up of particles with different sizes and shapes with a clear tendency of elongation. In contrast to the cases of Co/Cu and Co/Au, the fringes are not so well defined for Co/Ag. While keeping a general layered aspect, they are more randomly distributed [Fig. 1(b)] than in the other samples. In spite of this more disordered arrangement, the clusters are well detached from one another. [Fig. 2(b)]. The average diameter of the particles ranges between 3 and 5 nm.

In order to get more structural information, a high resolution transmission electron microscopy (HRTEM) study was done. In all three cases, HRTEM images [Figs. 2(a)–2(c)] reveal the crystalline nature of the particles, within the dark fringes for Co/Cu and Co/Au, and the dark particles in Co/Ag, while they show the amorphous character of the bright fringes. The elongated shapes inferred at low magnification can be understood as a consequence of the particles superposition along a row. This can be better observed in Fig. 2(a) corresponding to the external layer of the Co/Au film where the particle concentration decreases.

The analysis of the chemical composition by means of EDX analysis indicates the coexistence of the two elements in the Co/Cu, Co/Ag, and Co/Au samples. However, the spot resolution is not sufficient to resolve the localization of Co and the metal. In some particles, a light gray aura seems to surround the darker gray core, while inside the Co/Cu layers, near the thinner border of the TEM sample, a lighter gray band connects the darker particle spots. Both lighter gray bands could be indicative of the noble metal surrounding the Co particle. Figures 3(a)–3(c) are magnified HRTEM images of individual particles of the Cu, Ag, and Au samples, respectively, and include the corresponding fast Fourier transform (FFT). In all of the three cases, the measured periodicities in the images as well as the distances and angles on the FFT are in agreement with a fcc lattice along $[10\bar{1}]$ zone axis. The splitting of the spots in some cases indicates the

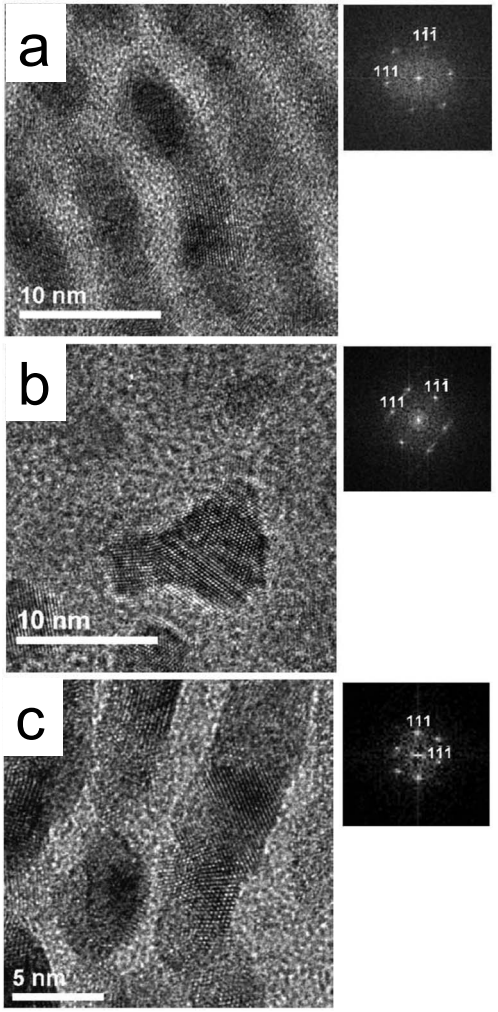

FIG. 3. HRTEM images of Co particles along the $[10\bar{1}]$ zone axis in the same samples as in Fig. 2: (a) Cu, (b) Ag, and (c) Au capped. The corresponding Fourier transforms (FFTs) are shown. In (a)–(c), the particle core crystal structure is fcc. It is not possible to discern the Co from the metal capping, since the latter has similar interatomic distances and also crystallize in the fcc structure. In the Co/Au, it was possible to discern some twinned zones. In (b), the faceted shape of the particle is evidenced and in FFT the spots of the twinned structures are labeled.

presence of twinning in the particle [Fig. 3(c)]. This can indeed also be observed in those particles where two orientations are evident. On the other hand, there is no clear evidence of a formation of a new intermetallic compound.

The overall picture in the three studied samples is that the Co particles are surrounded by the capping layer that acts like a matrix, completely covering the particles. The regularity found in the alumina-capped sample, i.e., with alumina as a matrix, is less clear in these samples. However, most of the particles seem to be detached from one another or connected within the layer by the noble metal. From the HRTEM, it was not possible to discern the interface between the Co particle and the capping metal because of the common fcc structure and the similarity in interatomic distances. The particles are not spherical, but irregular. In view of the HRTEM images in Fig. 3, where the crystallinity of the Co core particles is evidenced, the possibility that the particles are faceted is large.

Magnetic measurements performed on the $t_{Co}=0.7$ nm samples enabled us to determine their blocking temperatures T_B. These data for Co/Al_2O_3, Co/Cu, and Co/Au were given elsewhere.[6] In this paper, data for the Co/Ag samples are first reported, and it is nice to verify that the trend followed is that of alumina $<$Cu$<$Ag$<$Au capped (see Table I). Moreover, K_{eff} for the four systems also follows the same trend in increasing values. The surface anisotropy K_S deduced from the experimental results after applying Eq. (1) with $\langle D\rangle=3$ nm are included in Table I. The increase in anisotropy with capping and a decrease in average diameter, as described in Ref. 6 for the Co/Al_2O_3, Co/Cu, and Co/Au cases, are also verified by Co/Ag, being intermediate with respect to Co/Cu and Co/Au, as could be expected from electronic considerations (see below).

IV. X-RAY MAGNETIC CIRCULAR DICHROISM IN CAPPED SAMPLES

The XMCD technique may give some direct evidence on the hybridization of the interatomic 3*d*-*nd* and the Co intraatomic 3*d*-4*p* bands. In this section, the results on the Co *K* and Co, Cu, Ag, and Au $L_{2,3}$ edges are presented for the alumina-capped and the three metal-capped samples.

From a XMCD experiment at the $L_{2,3}$ edges of Co, Cu, Ag, or Au, one obtains, through the sum rules,[20,21] the spin and orbital moments averaged over the core and the surface of the particle and the number of holes n_h in the empty exchange split *nd* subbands. The sum rules have been applied to the spectra to derive the orbital, spin, and total magnetic moments, and the symbols and sign criteria defined in Ref. 22 have been used below. The constant $C=(I_{L_2}+I_{L_3})/n_h$, where $I_{L_2}+I_{L_3}$ are the white-line integrated intensities after subtraction of the contributions from transitions to the continuum, and n_h, depend on the normalization method used for the XAS spectra. Therefore, in this paper, all the experimental data show not only the XAS but also the normalized data, and the values of C are explicitly given. For the sake of comparison, we have adopted the normalization procedure for each metal as that found in literature. It was not possible to derive the integrated XAS white-line intensity from our measurements, since the difference in the XAS spectra of the present samples with that of the corresponding bulk metal is inappreciable. Therefore, to obtain the magnetic moments, the method first proposed in Ref. 9 has been employed.

It is noteworthy that in the present case of particles, with their anisotropy axes oriented at random, the dipolar term m_D cancels out so that the sum rule $(A-2B)=-Cm_S/\mu_B$ yields the spin component m_S. A and B are the integrated areas of the L_3 and L_2 XMCD peaks, respectively. In Figs. 7–9, the parameters $p=A$ and $q=A+B$ have been depicted. Besides, m_L/m_S is directly derived from the ratio of the sum rules, which is independent of n_h and of the normalization method used.

To systematize the discussion, the results obtained for one particle size, namely, $\langle D\rangle\approx 3$ nm, are compared unless otherwise explicitly stated. In the experiments, a magnetic field

TABLE I. Blocking temperature T_B, effective volume anisotropy constant K_{eff}, surface anisotropy constant K_S obtained from K_{eff} with Eq. (1), and $D=3$ nm, which is determined from magnetic measurements. m_L, m_S, and m_L/m_S for the Co and noble metal atoms indicated in the left column, as determined from XMCD measurements. For the fcc bulk Co, $m_L/m_S=0.078$ (Ref. 27), and for all Co, $m_S=1.62\mu_B$ (Ref. 25).

	Al_2O_3 cap	Cu cap	Ag cap	Au cap
T_B (K)	30.1(1)[a]	35.0(1)[a]	37.0	43.0(1)[a]
K_{eff} (10^4 J/m^3)	53.(5)[a]	78.(10)[a]	110.(6)	139.(7)[a]
K_S (10^{-5} J/m^2)	23.2(2)	35.8(3)	51.5(4)	66.0(5)
Co 3*d*				
m_L/m_S	0.129(10)[a]	0.156(20)[a]	0.163(10)	0.197(10)[a]
m_L (μ_B)	0.209(16)	0.253(30)	0.264(16)	0.319(16)
$(m_L/m_S)_{\text{surf}}$	0.224(20)	0.301(30)	0.321(20)	0.419(30)
Co 4*p*				
m (μ_B)	−0.087(4)	−0.072(4) [b]	−0.078(4)	−0.072(4)
M n*d*				
m_L^{nd}/m_S^{nd}		0.32(3)	0.045(5)	0.10(5)[a]
m_L^{nd} (μ_B)		$10(3)\times10^{-4}$	$7(1)\times10^{-4}$	$1.5(5)\times10^{-3}$
m_S^{nd} (μ_B)		0.010(3)	0.014(3)	0.015(1)
m^{nd} (μ_B)		0.011(3)	0.015(3)	0.016(1)
M 4*p*				
m^{4p} (μ_B)		−0.016(2) [b]		

[a]Reference 7.
[b]Reference 5.

of 1 T is applied, which is sufficient to saturate the particle spin magnetization, but the paramagnetic moment contribution from x_{para} is negligible.

Under an applied field that saturates the particle magnetization ($H \geq 1$ T), the surface Co spin moment, which is isotropic, easily orients along the field, but the surface orbital moment gradually tilts from the direction normal to the particle surface to the direction of the applied field. The magnetic anisotropy energy associated with spin-orbit coupling is about 2 orders of magnitude larger than the dipole interaction, but the crystalline anisotropy is of the order of the s.o. coupling, so the spin and orbital moments are not parallel except when the field is parallel to the local easy axis of magnetization.[22] The projection of the orbital moment along the applied field direction m_L, which is averaged over all the surface of the particle, yields the mean orbital moment in the field direction. Therefore, the contribution of the orbital moment to the XMCD signal is the averaged projection of the local moments in the direction of the applied field (parallel to the photon beam direction in the experiments). If the particle is approximated to a sphere, the averaged orbital moment is

$$m_L = \frac{1}{3}(m_L^{\perp} + 2m_L^{\parallel}), \tag{2}$$

where $m_L^{\perp}$ is the orbital contribution normal to the particle surface and $m_L^{\parallel}$ is parallel to it. In the case of other particle shapes, the proportions of $m_L^{\parallel}$ to $m_L^{\perp}$ may be different.

A. X-ray magnetic circular dichroism at the Co *K* edge

The XMCD measurements at the Co *K* edge yield the magnetic moment of the 4*p* band (hybridized *sp* conduction bands). In Fig. 4, the collected spectra of the XMCD peaks are shown. The shape and amplitude of the measured peaks are similar to those of metallic Co.[10,23] The nonzero signal reflects the spin-dependent polarization caused by the exchange polarized 3*d* band by intraatomic hybridization. The sign of the XMCD spectra at the Co *K* edge is the same as in Ref. 10, where the Co/Cu multilayer has been studied in detail. This result indicates that the coupling between 4*p* and 3*d* levels of Co is antiferromagnetic.

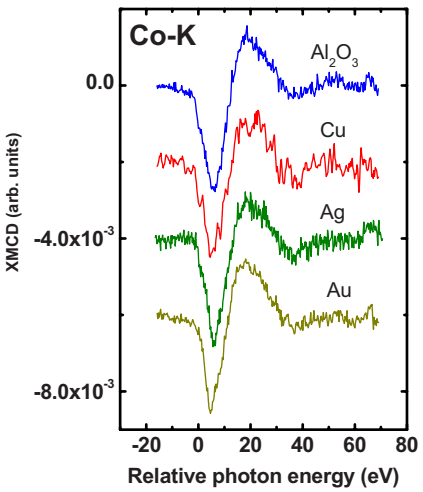

FIG. 4. (Color online) Co *K*-edge XAS spectra obtained at $T=5$ K and under a field of 1 T for the capped samples (blue: Co/Al_2O_3), (red: Co/Cu), (green: Co/Ag), and (yellow: Co/Au) for particles with the same $t_{Co}=0.7$ nm.

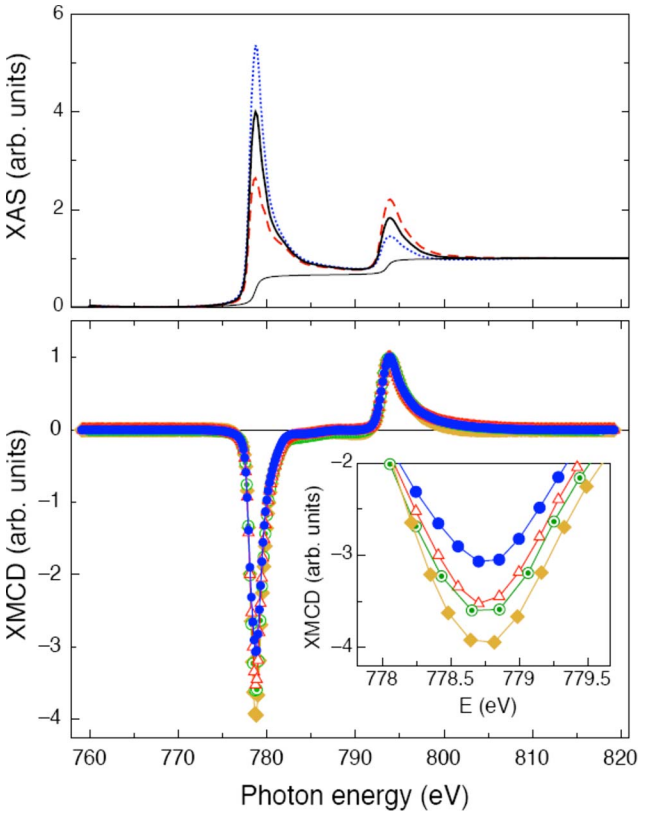

FIG. 5. (Color online) Co $L_{2,3}$-edge spectra of the same samples measured at $T=5$ K, $\mu_0 H=1$ T and incident angle 15°. (a) XAS spectra with positive helicity of the incoming beam (···), negative helicity (- - -), and mean curve (—). The two-step function used is also indicated (–). (b) XMCD spectra normalized to a common L_2 peak intensity, [(blue ●) Co/Al_2O_3] [(red Δ) Co/Cu], [(green ●) Co/Ag], and [(yellow ♦) Co/Au], for particles with the same $t_{Co}=0.7$ nm. Inset: expanded view of the L_3 peak minima. Note the increase in L_3 dichroic intensity in the trend alumina $<$Cu$<$Ag$<$Au capped.

From the comparison of the amplitudes of the XMCD Co *K*-edge spectra, it was derived that the Co moment in the alumina-capped Co particle is about 20% larger than the one found for the three Co-capped ones. This implies that the number of electrons in the Co 4*p* band is reduced through contact with the capping metals; i.e., there is hybridization, and on average, it gives rise to a redistribution of electrons at the surface Co atoms. The x_{para} fraction of the Co atoms does not contribute to the XMCD signal in a significant way.

B. X-ray magnetic circular dichroism at the Co $L_{2,3}$ edges

The experimental XMCD spectra at the Co $L_{2,3}$ edges for the alumina-, Cu-, Ag-, and Au-capped Co particles are depicted in Fig. 5, together with one example of XAS, for the sake normalization. The XMCD data normalized to the XMCD L_2 peak are shown to highlight the increasing trend of the L_3 peak intensity, which, in turn, reflects the increase in m_L/m_S with the capping of Cu, Ag, and Au. The ratios derived from the measurements for the alumina-, Cu-, Ag-, and Au-capped samples have values that span from 0.129 for the alumina-capped to 0.197 for the Au-capped Co particles, as shown in Table I.

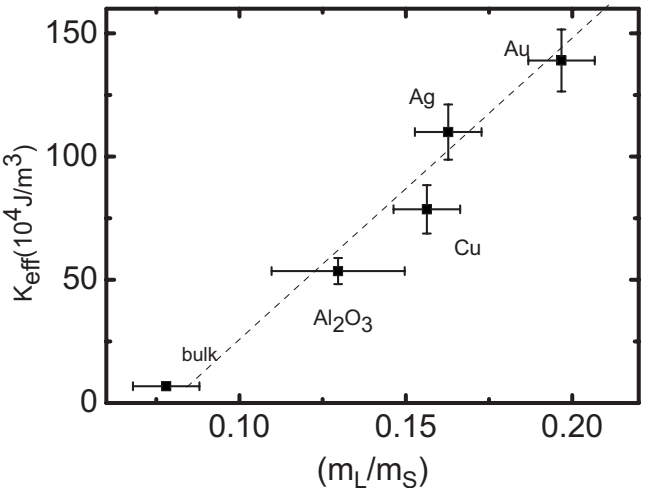

FIG. 6. K_{eff} as a function of m_L/m_S for alumina, Cu-, Ag-, and Au-capped samples. The values for the bulk are included (Ref. 27). The dashed line is a linear fit to the data.

In Fig. 6, K_{eff} values are shown together with the values of m_L/m_S for samples with the same $t_{Co}=0.7$ nm, finding an excellent linear correlation between these two quantities. The extrapolation of this line nicely gives the measured K_{eff} and m_L/m_S for the bulk fcc Co.[24–26] This result clearly indicates that the orbital moment and magnetic anisotropy are related to the capped particles; i.e., the modification of the Co average orbital moment due to the interfacial interactions gives rise to an increase in the average effective anisotropy of the particle. Previously, a linear dependence between m_L/m_S and K_{eff} was found for particles differing just on the average size in Co particles deposited on Pt (Ref. 3) and in the Co particles embedded in alumina.[4] Just as for Co thin films,[8] the correlation between K_{eff} and m_L/m_S seems to be a general rule in nanoparticles.

At any rate, the enhancement of m_L/m_S is larger in nanoparticles than in thin films. For example, a maximum value of $m_L/m_S=0.12$ was found for about 5 monolayers of Co deposited on Cu (Ref. 27); the same value, as maximum, was found in the case of four Co atomic layers in a stair case layer of Co sandwiched between Au.[8] The same value was found again in islands of two Co monolayer thickness deposited on Au.[28]

Although the integrated areas $I_{L_2}+I_{L_3}$ of the alumina- and metal-capped samples should yield direct information on n_h for the Co 3*d* band, we found that experimental errors prevent determining coherent results. Therefore, we have adhered to the assumption that n_h depends on the element, and taken the calculated value for bulk Co, $n_h=2.49$.[9] The corresponding scaling constant for Co, deduced from $I_{L_2}+I_{L_3}=15.1(5)$ is $C=60(2)\mu_B^{-1}$. Similar n_h values have been obtained from calculations for small Co clusters ($n_h=2.40$) (Ref. 3) or in Pt/Co multilayers ($n_h=2.45$).[29] The approximation that the value of m_S may be considered as varying little from the bulk value, $m_S=1.62\mu_B$ (Ref. 25) is applied in the rest of the paper. We find a justification to this approximation

in the fact that the average total moment of the Co atoms in the particles, as deduced from $M(H)$ measurements, is nearly that of the bulk, irrespective of capping or $\langle D \rangle$.[6]

Since XMCD is probing Co in clusters of similar average diameter, the number of surface and core Co atoms is the same in all four samples. Therefore, the increase in m_L/m_S with respect to the bulk as a function of capping exclusively reflects an increase due to the surface Co atoms. In the analysis of K_{eff}, the separation between surface and core atom contributions has been successfully applied to understand the enhancement of the surface anisotropy by capping.[6] A simple core shell model allows us to estimate the fraction of surface atoms with the formula $f=1-(1-0.4/D)^3$, with D (nm) ($f=0.35$ for $D=3$ nm) in the approximation of spherical fcc particles.[6] Within this model, $K_{\text{eff}}=K_{\text{bulk}}(1-f)+K_{\text{surf}}f$, where K_{surf} refers to the surface atoms, is approximately $K_{\text{eff}}=K_{\text{bulk}}+6K_S/D$ to within 10% at $D=3$ nm.

If we apply the same core shell model to the contributions to m_L/m_S, the contribution from surface atoms $(m_L/m_S)_{\text{surf}}$ may be deduced from the equation

$$\frac{m_L}{m_S}=\left(\frac{m_L}{m_S}\right)_{\text{bulk}}(1-f)+\left(\frac{m_L}{m_S}\right)_{\text{surf}}f, \tag{3}$$

where m_L/m_S is the measured value averaged over the Co mass forming the particles and $(m_L/m_S)_{\text{bulk}}=0.078(1)$ for fcc Co.[27] The resulting values for $(m_L/m_S)_{\text{surf}}$ have been included in Table I. The values that were found range from 0.224 for Co/Al_2O_3 to 0.419 for Co/Au; i.e., in the extreme case of Co/Au, the orbital moments at the surface atoms increase by a factor of 5 with respect to bulk fcc Co.

A highly enhanced orbital magnetism on Co cluster surfaces in a Cu matrix has been reported earlier.[30] These authors measured the Co $L_{2,3}$ edges and used a core shell model to deduce the surface orbital moment from their data, finding a value of $m_L/m_S=0.35$ at the Co surface monolayer, which is in good agreement with our result. Co particles supported on Au have also been measured, although of island or disklike shape, showing also a large increase in m_L/m_S with respect to the bulk value.[31]

The XAS branching ratio, which is defined as the ratio of intensities, $I_{L_3}/(I_{L_2}+I_{L_3})$ has been found not to depend on capping and has the value of 0.74(1). Since the branching ratio gives a measure of the angular part of the spin-orbit operator, it can be considered that this quantity remains unaltered by capping.[32]

C. X-ray magnetic circular dichroism at the $L_{2,3}$ edges of the noble metals

The capping metals Cu, Ag, and Au have $3d^{10}$, $4d^{10}$, and $5d^{10}$ bands, respectively. In the metallic state, as is our case, the bands are not completely filled, and, therefore, yield to a small but distinguishable white line in the XAS experiments. These metals are diamagnetic in the absence of hybridization with other elements and, therefore, give no XMCD signal. However, when in contact with other metals, in particular, ferromagnetic Co, hybridization between the conduction bands alters their number of holes, on one hand, and polarizes by exchange interaction those bands giving rise to the splitting into majority up (completely filled) and minority down (partially filled) spin states d bands, on the other hand. Then, in the first approximation, the magnetic moment is equal to the average number of electrons removed from the atom, i.e., the number of holes n_h. The changes in the occupation of the electronic orbitals give rise to a small but measurable induced magnetic moment in the capping metal layer. These effects have been found in Co thin films capped with Cu,[9] Ag,[11] and Au,[12] so the three noble metals are polarized by magnetic Co at the Co/M interfaces.

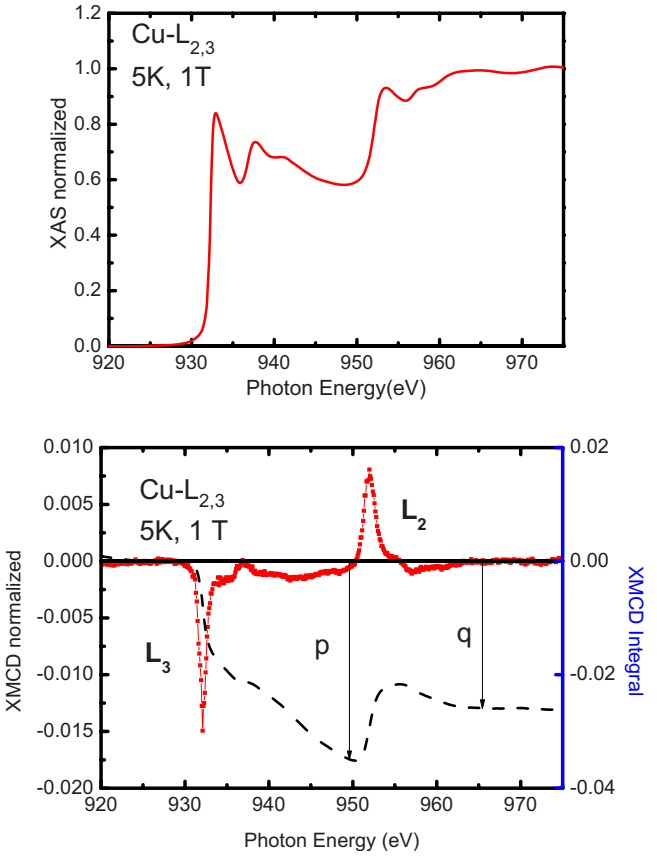

FIG. 7. (Color online) Normalized Cu $L_{2,3}$-edge XAS (top) and XMCD (bottom) spectra of $Si/Al_2O_3/(Co/Cu/Al_2O_3)\times 15/Al_2O_3$. (-) Area integral. The arrows indicate the higher limit of the p and q integrals.

To check whether this also holds for the Co granular capped samples, XMCD experiments at the $L_{2,3}$ edges of Cu, Ag, and Au have been performed. The measurements were done at $T=7$ K, an applied field of $\mu_0 H=1$ T, and an incidence angle of 75°. Indeed, Cu, Ag, and Au show nonzero XMCD signals, indicating that a fraction of the capping atoms become polarized by the exchange spin polarization with the Co moments (see Figs. 7–9).

For the XMCD analysis, we depict the areas subtended by the L_3 and L_2 peaks, as obtained from direct integration of the data. In the case of Cu, p has been taken at the energy of the minimum of the XAS spectra between the L_3 and L_2 peaks and q when the integral converges to a constant. For the Ag and Au cases, where the statistical scatter is larger, we give the integration of a smooth Lorentzian function as guide for the eyes, which fits the data for these two metal cappings,

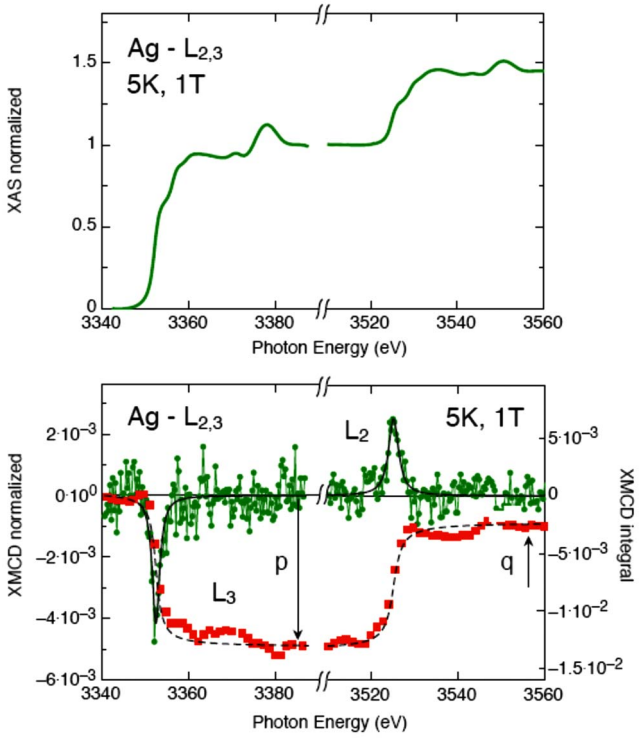

FIG. 8. (Color online) Normalized Ag $L_{2,3}$-edge XAS (top) and XMCD (bottom) spectra of $Si/Al_2O_3/(Co/Ag/Al_2O_3)\times 20/Al_2O_3$. (-) Fit to Lorentzian function. (■) Area integral; (--) area integral of the Lorentzian. The arrows indicate the higher limit of the p and q integrals.

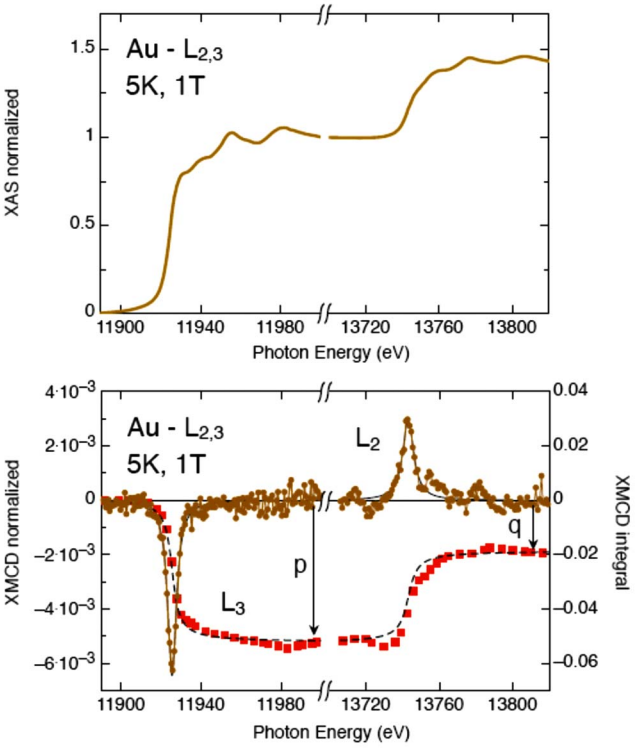

FIG. 9. (Color online) Normalized Au $L_{2,3}$-edge XAS (top) and XMCD (bottom) spectra of $Si/Al_2O_3/(Co/Au/Al_2O_3)\times 25/Al_2O_3$. (-) Fit to Lorentzian function. (■) Area integral; (--) Area integral of the Lorentzian. The arrows indicate the higher limit of the p and q integrals.

as shown in Fig. 8(b) for Ag and Fig. 9(b) for Au. The energies at which p and q have been taken are also shown in Figs. 8(bottom) and 9(bottom). The error in the integration is considered to be the width of its deviation with respect to the mean guideline and amounts to 15% and 10% in the Ag and Au cases, respectively.

The ratio m_L^{3d}/m_S^{3d} is directly obtained from the sum rules and is independent of any choice in the scaling constant. For Cu, $m_L^{3d}/m_S^{3d}=0.32(3)$, which is larger than the ratio found in other Co granular alloys in the presence of Cu [$m_L^{3d}/m_S^{3d}=0.018$ (Ref. 33)] and in a random $Co_{90}Cu_{10}$ alloy [$m_L^{3d}/m_S^{3d}=0.09$ (Ref. 9)]. However, the factors between n_h and the white-line area, given in Ref. 9, are $C=5.6\mu_B^{-1}$ and $14\mu_B^{-1}$ for the m_S^{3d} and m_L^{3d} sum rules, respectively (normalization of the total L_2 and L_3 XAS to 1), which yield to $m_S^{3d}=0.010(3)\mu_B$ and $m_L^{3d}=10(3)\times 10^{-4}\mu_B$. If this method is employed, the value for the ratio $m_L^{3d}/m_S^{3d}=0.10(3)$, which is quite low but comparable to other determinations. At any rate, the total moment $m^{3d}=0.011(3)\mu_B$ is deduced, while the orbital moment is very small and practically negligible. It is concluded without ambiguity that the Cu-capping layer is magnetically polarized by the Co particles. It is interesting to note that this value is in the range of the predicted polarization per Cu atom adjacent to a Co nanoparticle.[34]

In the case of the Ag-capped Co particles, a nonzero XMCD at the $L_{2,3}$ edges is observable (Fig. 8), although the signal is very small; the larger L_3 peak amounting to just a few per thousand of the XAS signal. Only the high quality of the ID12 beamline at the ESRF has allowed this experiment. The corrected data are shown in Fig. 8. The ratio $m_L^{4d}/m_S^{4d}=0.045(5)$ is extremely small, as compared to Cu (or Au, see later). Therefore, the detected nonzero induced magnetization can essentially be assigned to the spin component. The determination of the constant C was derived in Ref. 11 by obtaining the white-line excess area with respect to Ag, ΔA_{wl}, on one hand, and using the method described for the interpretation of the XAS data[35] to determine the increase in the number of holes in the sample (NiFe/Ag multilayers) Δn_h, with respect to a pure Ag sample, on the other. Then, finding the quotient $C=\Delta A_{\mathrm{wl}}/\Delta n_h=2.3(2)\mu_B^{-1}$. The value $m_S^{4d}=0.014(3)\mu_B$ is obtained, which is higher than that in Cu. This value can only be compared to $m^{4d}=0.0135\mu_B$ determined for Ag in $Ni_{81}Fe_{19}/Ag$ multilayers.[11] The value of $m_L^{4d}=7\times 10^{-4}\mu_B$ may be considered as negligible.

The XMCD data at the Au $L_{2,3}$ edges performed on the Au-capped Co nanoparticles also indicated that there is a nonzero magnetic moment induced by the hybridization with Co (Fig. 9). The obtained value is $m_L^{5d}/m_S^{5d}=0.10(5)$. This result is in reasonable agreement with the published value of $m_L^{5d}/m_S^{5d}=0.12$,[12] where the value $C=7.8\mu_B^{-1}$ was used to determine m_L^{5d} and m_S^{5d} of Au in a Co_{12}/Au_4 multilayer. To derive C, the values of I_{L_2} and I_{L_3} were experimentally determined from the white line of a reference Au_4Mn compound (XAS normalization of L_3 edge to 1 and of L_2 edge to 0.45) with respect to the bulk Au XAS signal and n_h from the difference in the calculated n_h values for Au_4Mn and bulk

Au. Using that constant, $m_S^{5d}=0.015(1)\mu_B$ and $m_L^{5d}=1.5(5)\times10^{-3}\mu_B$, yielding to a total of $m^{5d}=0.016(1)\mu_B$.

The three capping noble metals are, therefore, polarized by the Co magnetic moments. The negative sign of the L_3 peak and the positive sign of the L_2 one, which are the same as the $L_{2,3}$ peaks of Co on the same sample, temperature, and field, indicate that the coupling between the Co average moment and the moment induced in the noble metal is ferromagnetic. The same sign for this coupling had been found for Co thin films with Cu, Ag, or Au interfaces.[9,11,12]

The ratio m_L/m_S is free of any scaling procedure. It is directly deduced from the XMCD signal, therefore it only gives information on those M atoms that are magnetically polarized, i.e., those affected by the exchange field of the magnetic Co. The M atoms outside of the sphere of influence of Co are silent to the XMCD, although they give a contribution to the XAS signal that may hamper the correct determination of the scaling factor C (see below). The fact that the ratio m_L^{nd}/m_S^{nd} in the three cases studied here have values similar to those found in other cases of the same M in contact with Co indicates that this is directly related to the degree of hybridization of the $3d$ of Co with the nd electron band of M at the interface. Thus, it is an intrinsic property related to the two metals involved at the interface.

Besides, the only case in which the presence of an induced orbital moment in the capping metal is unambiguously proven is the Au-capped sample. The spin-orbit coupling constants are $\zeta_d=60$, 97, 272, and 608 meV for Co, Cu, Ag, and Au, respectively,[36] so the larger m_L^{nd} induced in Au is probably associated with this larger s.o. coupling with respect to the other metals.

Another nice result is that m^{nd} increases in the trend Cu, Ag, and Au cappings. This may be related to two mechanisms, an increasing number of holes in the nd and nsp bands of the noble metal, since they may also play a role in the hybridization with the $3d$ band of Co, or an increased exchange polarization of those bands. Each may give rise to the presence of induced moment, independently, although most probably both mechanisms are acting together in this case. Unluckily, the possible variation of n_h could not be derived from the direct detection of an increased white line in these M-capped Co particles with respect to the bulk corresponding M noble metal, since the error bar in our XAS data does not support this analysis.

In the case of Au capping, the Au $L_{2,3}$-edge experiments were also performed on a sample with a smaller diameter, $\langle D\rangle=1.8$ nm, corresponding to $t_{\mathrm{Co}}=0.4$ nm. The XMCD signals are smaller than those for $t_{\mathrm{Co}}=0.7$ nm and $\langle D\rangle=3$ nm. Since the XMCD spectra in both cases are scaled to the $L_{2,3}$-edge XAS spectra and the XAS spectra for the two samples are indistinguishable, this implies that the relative number of Au atoms influenced by the Co exchange field is smaller in the case of the sample with smaller Co particles. From the analysis of the Au $L_{2,3}$ XMCD data (Fig. 10), it is found that m_L^{5d}/m_S^{5d} is identical for $t_{\mathrm{Co}}=0.4$ and 0.7 nm, while the total magnetizations per Au atom are $m=0.005\mu_B$ and $0.017\mu_B$, respectively, that is, they differ markedly, being $r_{\mathrm{Au}}^{L_{2,3}}=m_{t\mathrm{Co}=0.4}/m_{t\mathrm{Co}=0.7}\approx0.32$ the ratio of polarized Au atoms in one sample with respect to the other. This result is unexpected, since the number of Co surface atoms which polarize

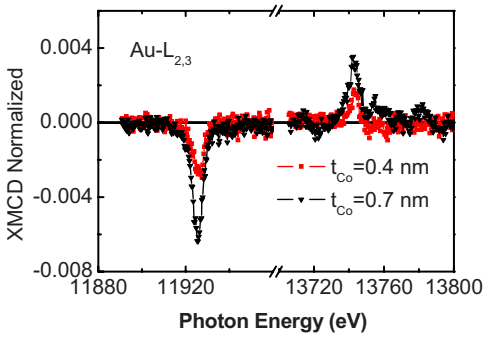

FIG. 10. (Color online) Au $L_{2,3}$-edge XMCD of $\mathrm{Si}/\mathrm{Al_2O_3}/(\mathrm{Co}/\mathrm{Au}/\mathrm{Al_2O_3})\times25/\mathrm{Al_2O_3}$: (■) $t_{\mathrm{Co}}=0.4$ and (▼) $t_{\mathrm{Co}}=0.7$ nm.

Au, with respect to the number of core Co atoms, is larger for the particles with smaller diameter. One needs to recollect that those Au atoms in contact with the paramagnetic fraction of the deposited Co are XMCD silent. Therefore, the number of polarized Au atoms is directly related only to the number of Co atoms at the surface of the particles. It is known that the polarization of the noble metal rapidly decays with distance from the interface,[9,11] being the first shell, and the one sustaining most of the polarized moment. Therefore, the simplification that

$$n_{\mathrm{Au}}^{\mathrm{polarized}}\approx n_{\mathrm{Co}}^{\mathrm{surf}} \tag{4}$$

is done. Here, the $n_{\mathrm{Co}}^{\mathrm{surf}}$ per unit area of the sample platelet may be estimated from the amount of nominal Co sputtered t_{Co}, the fraction of that Co which forms the particles $(1-x_{\mathrm{para}})$, and f as the fraction of the Co atoms in the particle that are located at the surface,

$$n_{\mathrm{Co}}^{\mathrm{surf}}=t_{\mathrm{Co}}(1-x_{\mathrm{para}})f. \tag{5}$$

The ratio of $n_{\mathrm{Au}}^{\mathrm{polarized}}$ for the two particle sizes is

$$r_{\mathrm{Au}}=\frac{[t_{\mathrm{Co}}(1-x_{\mathrm{para}})f]_{t\mathrm{Co}=0.4}}{[t_{\mathrm{Co}}(1-x_{\mathrm{para}})f]_{t\mathrm{Co}=0.7}}=0.86\frac{(1-x_{\mathrm{para}})_{t\mathrm{Co}=0.4}}{(1-x_{\mathrm{para}})_{t\mathrm{Co}=0.7}}. \tag{6}$$

The parameter x_{para} has been determined for both samples from TEM measurements;[13] i.e., for $t_{\mathrm{Co}}=0.4$ nm sample, $x_{\mathrm{para}}=77\%$, and for $t_{\mathrm{Co}}=0.7$ nm sample $x_{\mathrm{para}}=45\%$, yielding the ratio $r_{\mathrm{Au}}=0.35$, which is in good agreement with the experimental ratio.

Thus, the strong reduction in r_{Au} may be explained as due, essentially, to the different amounts of x_{para} existent in each sample and not due to size effects associated with electronic confinement or depth dependent Co moments.

D. X-ray magnetic circular dichroism at the Cu *K* edge

With respect to the K edge of the three capping layer metals, only the XMCD at the Cu K edge could be measured.[5] Since this XMCD nonzero signal probes the $4p$ holes in the conduction band, this result indicates that the $4p$ states are hybridized with the Co $3d$ band holes, via exchange spin polarization, and become polarized antiparallel to the $3d$ moments. On the other hand, its sign is the same as that of the Co K-edge XMCD peak, indicating that the Cu $4p$

holes are ferromagnetically coupled to the Co $4sp$ conduction band holes. The mean $4p$ moment value found was $m^{4p}=-0.016(2)\mu_B$, antiparallel to the Co $3d$ moment and, therefore, parallel to the Co $4p$ moment.[5]

V. DISCUSSION

The results shown in Sec. I and IV indicate that the electronic structure of the Co atoms at the Co/M interface governs the particle magnetic properties. Indeed, an increasing K_{eff} and, correspondingly, K_S are found in the trend alumina, Cu, Ag, and Au caps. On the other hand, a simple evaluation of the orders of magnitude of the anisotropies involved, magnetocrystalline, shape, or stress, supports the fact that none of them can explain the observed increase in K_{eff} with respect to the bulk value, even in the case that the particles were needle shaped.[7]

As a rough approximation, the Co particles in the M-capped samples have been considered as spheres of average diameter $\langle D\rangle$. However, HRTEM pictures show that the particles are not spherical but irregular, and it can be conjectured from the well oriented crystal lattice in the core that the particles are probably faceted. In fact, recent calculations of the anisotropy energy in Co faceted, nonregular polyhedra have given K_{eff} values in good agreement with our data for the alumina-capped particles.[37] The Co/M interface probably consists of planar facets of limited dimensions. Therefore, as a guidance, it is reasonable to pay attention to the electronic modifications of Co at the surface of planar Co/M thin films, implicitly two dimensional, for which there exist theoretical and experimental results as to how the Co surface anisotropy is modified by the interfacial metal.

Several calculations of the Co thin film interface anisotropy energy have been performed. A freestanding Co monolayer is predicted to have parallel anisotropy, i.e., negative magnetic anisotropy energy (MAE),[38] but capping with Cu, or with 1 monolayer of Au increases the MAE; i.e., it approaches zero, but the anisotropy remains planar.[39,40] However, in a Cu/Co/Cu sandwich, i.e., with another Cu capping layer, a positive shift of the anisotropy to nearly zero or even weakly positive MAE[38] is induced. Moreover, capping with more than 2 monolayers of Au changes the Co anisotropy to perpendicular.[40] According to the approach in Ref. 38, the trend of the positive shift in the MAE should be increasing as Co/Cu, Co/Ag, and Co/Au. However, the predicted MAE for Co/Cu and Co/Ag is negative and a conflicting theoretical result states that the MAE in Cu/Co/M-capped sandwiches favors perpendicular anisotropy for M=Cu and Ag, while favors basal for Au.[41]

The MAE crossover from negative to positive as a function of thickness and Au capping has been nicely explained in terms of the following simple model.[42] At the interface, the Co atoms are bonded with one another by the same interactions as in the bulk, on one side, while the Co-M interactions are evidently different on the other. The case of $3d$ in-plane and out-of-plane bands is then separately considered. In agreement with the above in-plane and out-of-plane band models, the in-plane band remains identical to the bulk, while the out-of-plane band is modified, giving rise to the surface anisotropy. It was shown that the MAE depends on the in-plane and out-of-plane $3d$ bandwidths. This is so because the Co orbital moment mainly arises from the minority band since the majority band has no net orbital moment and the average bandwidth determines the average separation of the filled and empty minority band states. The magnetic surface anisotropy originates from the spin-orbit coupling of occupied and unoccupied states of the minority band. The dominant term in the MAE is, therefore, the spin-orbit second order perturbation term,

$$\Delta E_{\text{s.o.}} \approx \xi^2 \sum_{u,o} \frac{|\langle u|L_z|o\rangle|^2 - |\langle u|L_x|o\rangle|^2}{\varepsilon_u - \varepsilon_o}, \tag{7}$$

where u and o represent unoccupied and occupied spin-down states and ξ is the spin-orbit coupling constant.[38] When the coupling through L_z is stronger, the MAE becomes positive and the system presents perpendicular anisotropy.[42] Therefore, the induction of magnetic anisotropy depends on ξ of Co and on the actual states that have a probability of mixing; the smaller the difference in energy, the larger the MAE is. Within this scheme, the positive shift of MAE would be related to the decreasing difference in the d orbital energy of the Co and the capping atom. Since these energy differences are −2.37, −1.44, and −0.21 eV for Cu, Ag, and Au, respectively, the trend of increasing MAE that is expected to follow is Co/Cu < Co/Ag < Co/Au. The same concepts may be extrapolated to the Co/M interfaces at the polyhedron facets of the irregular Co particles. Therefore, one could expect an increasing surface anisotropy in those facets following the trend alumina, Cu, Ag, and Au capped.

Very enlightening in understanding the particle uniaxial anisotropy are the calculations of MAE for a Co cluster built by successively adding pairs of layers, with one at each side. Although the starting finite Co monolayer has planar anisotropy, just as an infinite monolayer Co thin film, the MAE decreases as facets grow from each side until it changes sign, i.e., the particle becomes uniaxial when two facets are added to the closed shell cluster.[37] This mechanism may be classified as shape anisotropy. Superimposed to this mechanism is the interaction with the matrix which will add a positive shift to the MAE of the facets following the trends Co/alumina, Co/Cu, Co/Ag, and Co/Au and thus qualitatively explaining our observation. The fact that capping with Cu already increases K_{eff} in our sample is relevant, since this implies that the predominant anisotropy is always positive. Indeed, if the surface MAE of the Co/Al_2O_3 particle had been negative, the capping with Cu would have implied a compensation of MAE and, consequently, a decrease in K_{eff}, which is contrary to our experimental result. With respect to the Cu capping, our experimental result also seems to contradict the reduction in MAE that was predicted in the calculations for closed shell Co clusters with Cu additional facets or embedded in Cu.[34,37]

From the above arguments, one concludes that the relative increase in MAE with respect to the Co vacuum interface when capping in the trends Cu, Ag, and Au gives rise to an increase in the surface perpendicular anisotropy by an increase in the bond strengths with the interfacial atoms and a

broadening of the out-of-plane d electron minority band while keeping the in-plane band unmodified. The effect is a net increase in $m_L^{\perp}$, while $m_L^{\parallel}$ remains constant. Consequently, the absolute value of m_L should increase as well [Eq. (2)]. Ultimately, this would translate into an increase in K_S, after the simple but powerful relation proposed by Bruno[43] that correlates the orbital moment anisotropy (OMA) with the interface magnetocrystalline anisotropy energy (MAE),

$$\Delta E_{\text{s.o.}} \propto -\xi(m_L^{\perp} - m_L^{\parallel}) \propto -K_S, \tag{8}$$

where ξ is the Co spin-orbit coupling constant.

In a recent paper,[44] the limits of validity of this expression have been assessed in the case of a Co thin film with an interface of a different metal, in particular, Cu and Au. It is argued that Eq. (8) is well fulfilled in the case of a Co/Cu interface since the s.o. coupling of Cu is low. In contrast, they find that Eq. (8) may not hold in the case of a Co/Au interface since the Au s.o. coupling is large. However, no simple relationship between the MAE and OMA is given in that paper. At any rate, in the present work, we conjecture that Eq. (8) holds for the four Co/Cu, Co/Ag, and Co/Au particle interfaces and check later for the consistency of the results for the Co/Cu and Co/Au cases.

In our experiment, the separation between $m_L^{\parallel}$ and $m_L^{\perp}$ is not possible. However, from Eq. (2), one may obtain an approximate relation between both parameters for the spherical particle approximation, namely, $m_L^{\perp} = (3m_L - 2m_L^{\parallel})$. For a nonspherical particle, the constants may differ but the linear dependence is maintained. Therefore, K_S can be expressed in terms of m_L and $m_L^{\parallel}$. One can consider $m_L^{\parallel}$ to be identical to that of the bulk, m_L^{bulk}, since it is related to the Co-Co bonding within the Co surface atoms and their distances and interactions can be approximated to be those of the bulk. Substituting in Eq. (8), one obtains $K_S \propto (m_L - m_L^{\text{bulk}})$. The relative variation of K_S for a given capping with respect to the $\text{Co}/\text{Al}_2\text{O}_3$ alumina-capped K_S^{Al}, $\Delta K_S = K_S - K_S^{\text{Al}}$ can be expressed as

$$\frac{\Delta K_S}{K_S^{\text{Al}}} = \frac{(m_L/m_S)_{\text{surf}} - (m_L^{\text{Al}}/m_S)_{\text{surf}}}{(m_L^{\text{Al}}/m_S)_{\text{surf}} - (m^{\text{bulk}}/m_S)_{\text{surf}}}, \tag{9}$$

where $(m_L^{\text{Al}}/m_S)_{\text{surf}}$ is the averaged ratio of orbital moment with respect to the spin moment at the surface of the alumina-capped sample.

This relation holds under the assumption that m_S does not vary. In Fig. 11, the relative variation of K_S is plotted as a function of the relative variation of $(m_L/m_S)_{\text{surf}}$, both normalized to the values for $\text{Co}/\text{Al}_2\text{O}_3$. An increase in nearly a factor of 2 in $(m_L/m_S)_{\text{surf}}$, when capping with Au, induces an increase in K_S by nearly the same factor.

The correlation found is very satisfactory, as the relative variation of the two magnitudes proposed in Eq. (9) is nearly followed. The difference in slope of the linear dependence may result from the rough approximation implied in the application of Eq. (2), which is strictly valid for the spherical particle. At any rate, this result shows that the origin of the surface anisotropy is directly connected with the increase in $(m_L/m_S)_{\text{surf}}$, which is in agreement with Bruno's model.

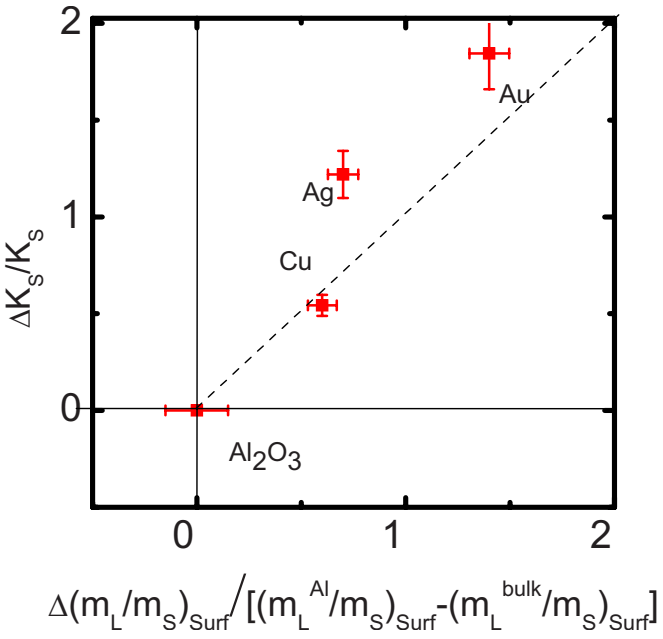

FIG. 11. (Color online) Dependence of the modification with capping of the surface anisotropy K_S and $(m_L/m_S)_{\text{surf}}$ relative to that of the alumina-capped case.

Evidently, the quantitative agreement relies on the conjecture that $m_L^{\parallel}$ remains constant, irrespective of the capping element. This conjecture is based on the similar assumption successfully applied in the analysis of Co thin films capped with noble metals such as Cu or Au.[22]

In the present study, the conjecture of fulfillment of Bruno's relation holds for the capped particles. This conclusion is in line with most previous work testing [Eq. (8)]. However, let us note that it is in contradiction with the predicted and found decrease in perpendicular anisotropy in the Co/Au interface in a Co thin film sandwiched between Au films.[44] The different topologies of particle and film probably play a role in this difference.

The increase in induced m^{nd} in Cu, Ag, and Au is probably caused by the corresponding increased polarizability in that trend. The spin-orbit coupling of the noble metal seems to play a second order role in this mechanism. It gives rise to an extra component to the orbital moment m_L^{nd} at the interfacial noble metal atom but is 2 orders of magnitude smaller than that of Co in the largest case, i.e., when $M = \text{Au}$.

The emerging interaction scheme at the Co/M interface is that, on one hand, the exchange polarized Co $3d$ band is antiferromagnetically coupled to the $4p$ band via intra-atomic spin-dependent hybridization and ferromagnetically coupled to the exchange split nd band of the M cap via $3d$-nd hybridization, on the other. In the case of Cu capping, there is evidence of the Cu $3d$ polarized band to be antiferromagnetically coupled to the $4p$ band via intra-atomic hybridization. Most probably, the $3d$ band of Co hybridizes with the $4p$ band of Cu, as proposed in Co/Cu thin films.[10]

In conclusion, the systematic increase in K_S with capping in the trends Cu, Ag, and Au has been correlated with the increase in the Co $3d$ mean m_L, which is caused by hybridization with the capping metal nd and $(n+1)p$ bands.

ACKNOWLEDGMENTS

This work has been partly funded by Grants No. MAT05-1272 and No. MAT05-02454 from MEC, and PM-012, IMANA, and CAMRADS from DGA. We thank Jesús González Casablanca for his valuable help with thin film preparation for TEM observation.

[1] F. Luis, J. M. Torres, L. M. García, J. Bartolomé, J. Stankiewicz, F. Petroff, F. Fettar, J. L. Maurice, and A. Vaures, Phys. Rev. B **65**, 094409 (2002).
[2] R. Yanes, O. Chubykalo-Fesenko, H. Kachkachi, D. A. Garanin, R. Evans, and R. W. Chantrell, Phys. Rev. B **76**, 064416 (2007).
[3] P. Gambardella, S. Rusponi, M. Veronese, S. S. Dhesi, C. Grazioli, A. Dallmeyer, I. Cabria, R. Zeller, P. H. Dederichs, K. Kern, C. Carbona, and H. Brune, Science **300**, 1130 (2003).
[4] F. Bartolomé, F. Luis, F. Petroff, L. M. García, J. Bartolomé, V. Cros, and H. Jaffres,J. Magn. Magn. Mater. **272-276**, e1275 (2004).
[5] L. M. García, F. Bartolomé, J. Bartolomé, F. Luis, F. Petroff, C. Deranlot, F. Wilhelm, A. Rogalev, P. Bencok, and N. B. Brookes, J. Magn. Magn. Mater. **316**, e23 (2007).
[6] F. Luis, J. Bartolomé, F. Bartolomé, M. J. Martinez, L. M. García, F. Petroff, C. Deranlot, F. Wilhelm, and A. Rogalev, J. Appl. Phys. **99**, 08G705 (2006).
[7] F. Luis, F. Bartolomé, F. Petroff, J. Bartolomé, L. M. García, C. Deranlot, H. Jaffrès, M. J. Martínez, P. Bencok, F. Wilhelm, A. Rogalev, and N. B. Brookes, Europhys. Lett. **76**, 142 (2006).
[8] D. Weller, Y. Wu, J. Stöhr, M. G. Samant, B. D. Hermsmeier, and C. Chappert, Phys. Rev. B **49**, 12888 (1994).
[9] M. G. Samant, J. Stöhr, S. S. P. Parkin, G. A. Held, B. D. Hermsmeier, F. Herman, M. van Schilfgaarde, L.-C. Duda, D. C. Mancini, N. Wassdahl, and R. Nakajima, Phys. Rev. Lett. **72**, 1112 (1994).
[10] S. Pizzini, A. Fontaine, Ch. Giorgetti, E. Dartyge, J. F. Bobo, M. Piecuch, and F. Baudelet, Phys. Rev. Lett. **74**, 1470 (1995).
[11] N. Jaouen, F. Wilhelm, A. Rogalev, J. M. Tonnerre, T. K. Johal, and G. van der Laan, IEEE Trans. Magn. **41**, 3334 (2005); N. Jaouen, F. Wilhelm, A. Rogalev, J. Goulon, L. Ortega, J. M. Tonnerre, B. Rodmacq, and A. Yaresko, J. Phys.: Condens. Matter **20**, 095005 (2008).
[12] F. Wilhelm, M. Angelakeris, N. Jaouen, P. Poulopoulos, E. Th. Papaioannou, Ch. Mueller, P. Fumagalli, A. Rogalev, and N. K. Flevaris, Phys. Rev. B **69**, 220404(R) (2004).
[13] J. Briático, J. L. Maurice, J. Carrey, D. Imhoff, F. Petroff, and A. Vaures, Eur. Phys. J. D **9**, 517 (1999).
[14] J. L. Maurice, J. Briático, J. Carrey, F. Petroff, L. F. Schelp, and A. Vaurès, Philos. Mag. A **79**, 2921 (1999).
[15] D. Babonneau, F. Petroff, J.-L. Maurice, F. Fettar, and A. Vaures, Appl. Phys. Lett. **76**, 2892 (2000).
[16] T. Saito, T. Katayama, Y. Kurosaki, M. Endo, S. Saito, T. Kamino, K. Kobayashi, Y. Suzuki, T. Nagahama, S. Yuasa, T. Koide, T. Shidara, H. Manaka, and H. Tokano, J. Magn. Magn. Mater. **272-276**, e1489 (2004).
[17] C. Morawe and H. Zabel, J. Appl. Phys. **77**, 1969 (1995).
[18] O. Kitakami, H. Sato, Y. Shimada, F. Sato, and M. Tanaka, Phys. Rev. B **56**, 13849 (1997).
[19] J. Bartolomé, F. Bartolomé, L. M. García, F. Luis, F. Petroff, V. Cros, H. Jaffrès, and A. Vaurès, in *Smart Materials for Ranging Systems*, ARW NATO No. 4 edited by J. Franse, V. Eremenko, and V. Sirenko (Springer, 2006), p. 1.
[20] P. Carra, B. T. Thole, M. Altarelli, and X. Wang, Phys. Rev. Lett. **70**, 694 (1993).
[21] B. T. Thole, P. Carra, F. Sette, and G. van der Laan, Phys. Rev. Lett. **68**, 1943 (1992).
[22] J. Stöhr, J. Electron Spectrosc. Relat. Phenom. **75**, 253 (1995).
[23] J. P. Rueff, R. M. Galera, C. Giorgetti, E. Dartyge, C. Brouder, and M. Alouani, Phys. Rev. B **58**, 12271 (1998).
[24] J. M. Torres, F. Luis, L. M. García, J. Bartolomé, J. Stankiewicz, F. Petroff, F. Fettar, and A. Vaurés, J. Magn. Magn. Mater. **242-245**, 575 (2002).
[25] C. T. Chen, Y. U. Idzerda, H.-J. Lin, N. V. Smith, G. Meigs, E. Chaban, G. H. Ho, E. Pellegrin, and F. Sette, Phys. Rev. Lett. **75**, 152 (1995).
[26] W. A. Sucksmith and J. E. Thompson, Proc. R. Soc. London, Ser. A **225**, 362 (1954).
[27] M. Tischer, O. Hjorstam, D. Arvanitis, J. H. Dunn, F. May, K. Baberschke, J. Trygg, J. M. Wills, B. Johansson, and O. Eriksson, Phys. Rev. Lett. **75**, 1602 (1995).
[28] T. Koide, H. Miyauchi, J. Okamoto, T. Shidara, A. Fujimori, H. Fukutani, K. Amemiya, H. Takeshita, S. Yuasa, T. Katayama, and Y. Suzuki, Phys. Rev. Lett. **87**, 257201 (2001).
[29] N. Nakajima, T. Koide, T. Shidara, H. Miyauchi, H. Fukutani, A. Fujimori, K. Iio, T. Katayama, M. Nývlt, and Y. Suzuki, Phys. Rev. Lett. **81**, 5229 (1998).
[30] D. A. Eastham and J. W. Kirkman, J. Phys.: Condens. Matter **12**, L525 (2000).
[31] H. A. Dürr, S. S. Dhesi, E. Dudzik, D. Knabben, G. van der Laan, J. B. Goedkoop, and F. U. Hillebrecht, Phys. Rev. B **59**, R701 (1999).
[32] B. T. Thole and G. van der Laan, Phys. Rev. A **38**, 1943 (1988).
[33] A. García Prieto, M. L. Fdez-Gubieda, J. Chaboy, M. A. Laguna-Marco, T. Muro, and T. Nakamura, Phys. Rev. B **72**, 212403 (2005).
[34] Y. Xie and J. A. Blackman, Phys. Rev. B **66**, 155417 (2002).
[35] A. N. Mansour, J. W. Cook, Jr., and D. E. Sayers, J. Phys. Chem. **88**, 2330 (1984).
[36] M. Vijayakumar and M. S. Gopinathan, J. Mol. Struct.: THEOCHEM **361**, 15 (1996).
[37] Y. Xie, and J. Blackman, J. Phys.: Condens. Matter **16**, 3163 (2004).
[38] D. S. Wang, R. Wu, and A. J. Freeman, J. Magn. Magn. Mater. **129**, 237 (1994).
[39] R. Wu and A. J. Freeman, J. Magn. Magn. Mater. **200**, 498 (1999).
[40] B. Újfalussy, L. Szunyogh, P. Bruno, and P. Weinberger, Phys. Rev. Lett. **77**, 1805 (1996).
[41] L. Szunyogh, B. Újfalussy, U. Pustogowa, and P. Weinberger, Phys. Rev. B **57**, 8838 (1998).
[42] J. Stöhr, J. Magn. Magn. Mater. **200**, 470 (1999).
[43] P. Bruno, Phys. Rev. B **39**, 865 (1989).
[44] C. Andersson, B. Sanyal, O. Eriksson, L. Nordström, O. Karis, D. Arvanitis, T. Konishi, E. Holub Krappe, and J. H. Dunn, Phys. Rev. Lett. **99**, 177207 (2007).